Nanoscale

PAPER

View Article Online
View Journal | View Issue

Cite this: *Nanoscale*, 2015, **7**, 15341

A novel form of β-strand assembly observed in $A\beta_{33-42}$ adsorbed onto graphene†

Xiaofeng Wang,[a] Jeffrey K. Weber,[b] Lei Liu,[c,d] Mingdong Dong,[d] Ruhong Zhou*[b,e,f] and Jingyuan Li*[a]

Received 25th January 2015,
Accepted 25th August 2015

DOI: 10.1039/c5nr00555h

www.rsc.org/nanoscale

Peptide assembly plays a seminal role in the fabrication of structural and functional architectures in cells. Characteristically, peptide assemblies are often dominated by β-sheet structures, wherein component molecules are connected by backbone hydrogen bonds in a parallel or an antiparallel fashion. While β-rich peptide scaffolds are implicated in an array of neurodegenerative diseases, the mechanisms by which toxic peptides assemble and mediate neuropathic effects are still poorly understood. In this work, we employ molecular dynamics simulations to study the adsorption and assembly of the fragment $A\beta_{33-42}$ (taken from the Aβ-42 peptide widely associated with Alzheimer's disease) on a graphene surface. We observe that such $A\beta_{33-42}$ fragments, which are largely hydrophobic in character, readily adsorb onto the graphitic surface and coalesce into a well-structured, β-strand-like assembly. Strikingly, the structure of such complex is quite unique: hydrophobic side-chains extend over the graphene surface and interact with adjacent peptides, yielding a well-defined mosaic of hydrophobic interaction patches. This ordered structure is markedly depleted of backbone hydrogen bonds. Hence, our simulation results reveal a distinct type of β-strand assembly, maintained by hydrophobic side-chain interactions. Our finding suggests the backbone hydrogen bond is no longer crucial to the peptide assembly. Further studies concerning whether such β-strand assembly can be realized in other peptide systems and in biologically-relevant contexts are certainly warranted.

Introduction

Amyloid formation exists at the nexus of a variety of neurodegenerative diseases.[1–5] Central to Alzheimer's disease, the amyloid β (Aβ) peptide (at 40–42 residues in length) is known to self-assemble into amyloid fibrils both in bulk solution and on the surfaces of cell membranes.[6] In general, the characteristics of peptide aggregates are diverse.[7] The polymorphism associated with amyloid formation has garnered growing interest due to a broad correlation between the presence of amyloids and cell death. Within most amyloid aggregates, component peptide segments become aligned in a β-strand topology, within which hydrogen bonds formed along the peptide backbone in either a parallel or an antiparallel motif.[8] It is well established that the ordered structures seen in β-sheet assemblies are cultivated by strong hydrogen bonds among backbone atoms. In other words, the backbone hydrogen bond is often considered to be crucial to peptide assembly. While the hydrophobic effect serves to drive peptide self-assembly, the question as to whether assembled peptide complexes can be preserved purely through hydrophobic interactions (in the absence of hydrogen bonds), to the best of our knowledge, remains unanswered. In particular, in assembly facilitated by a hydrophobic surface, one might imagine that hydrogen bonds could perform a muted part in maintaining structural integrity.

The adsorption and subsequent assembly of peptides (*e.g.* Aβ,[7,9–15] prion,[16,17] IAPP[14,17–19]) on surfaces associated with mica,[11,15,16,20] graphitic materials,[7,9–13,19–25] and self-assembled monolayers (SAMs)[10,14] has gained significant attention. Studies of peptide assembly on various materials promise to not only bolster understanding of peptide assembly mechanisms and their concomitant impacts on membrane structure,[26–30] but also help facilitate the application of peptide scaffolds to surface property modulation in materials science.[31–33] Along with intensive experimental studies,

[a]*CAS Key Laboratory for Biomedical Effects of Nanomaterials & Nanosafety, Institute of High Energy Physics, Chinese Academy of Sciences (CAS), Beijing 100049, China. E-mail: lijingyuan@ihep.ac.cn*
[b]*IBM Thomas J. Watson Research Center, Yorktown Heights, New York 10598, USA*
[c]*Institute for Advanced Materials, JiangSu University, Zhenjiang 212013, China*
[d]*Interdisciplinary Nanoscience Center (iNANO), Aarhus University, 8000 Aarhus C, Denmark*
[e]*Department of Chemistry, Columbia University, New York, New York 10027, USA*
[f]*Institute of Quantitative Biology and Medicine, SRMP and RAD-X, Soochow University, Suzhou 215123, China. E-mail: ruhongz@us.ibm.com*
†Electronic supplementary information (ESI) available. See DOI: 10.1039/c5nr00555h

molecular dynamics (MD) simulation techniques have been widely used to study the adsorption and assembly of peptides on surfaces.[10,12,17,19–22,34] As suggested by previous works, the proximity of a hydrophobic surface can serve to promote the peptide assembly process. Peptide adsorption is known to disrupt standard secondary structural formation, leading to an increased propensity for extended conformations on the surface. While adsorption supports an increase in the local peptide concentration, strong hydrophobic interactions with the surface can compete with hydrophobic interactions between adjacent molecules[12,22,35–37] and hinder the close packing of peptides needed for the formation of backbone hydrogen bonds. Despite the impact of surface interaction on the assembly process and its mesoscopic architecture,[7,10–12,38–40] the peptides are still connected by backbone hydrogen bonds.[38,40,41] Hence, these adsorbed peptide assemblies share the same structure features with "free standing" assemblies. However, as indicated in this work, surface interactions can even induce a non-canonical form of peptide assembly mainly maintained by hydrophobic side-chain interaction. In other words, our results suggest the backbone hydrogen bond is no longer crucial to the peptide assembly.

Recently, we characterized the assembly formed by the peptide fragment $A\beta_{33-42}$ when adsorbed onto a graphitic surface.[9] The $A\beta_{33-42}$ segment, in particular, is thought to be important to the formation of Aβ amyloid fibrils implicated in Alzheimer's disease.[8] In this work, we use MD simulations to study the adsorption and assembly of $A\beta_{33-42}$ onto graphene monolayers. As indicated in previous works,[11,12] graphitic surface can induce the adsorption of $A\beta_{1-42}$ peptides, facilitate the conversion to β-sheet structure, and serve as the template to promote peptide assembly. We find $A\beta_{33-42}$ can similarly adsorb onto the graphene surface and exhibit the tendency to extended structures. Strikingly, sufficiently strong hydrophobic interaction between graphene and $A\beta_{33-42}$ with largely hydrophobic amino acid sequence further induces the residual side-chains to stretch to both sides of the adsorbed peptides, and the resultant peptide assembly features a "mosaic" of hydrophobic interaction patches formed by a highly structured arrangement of aliphatic side-chains. Complementarity in size and shape of such hydrophobic side-chains thus appears to be important to the stability of this β-strand assembly. The importance of backbone hydrogen bonds to the peptide assembly has been well recognized, thus our current results should promote a better understanding of the molecular mechanisms of peptide assemblies. Furthermore, these findings of unique substrate-surface-peptide-monolayer structure may also help advance the nanotechnology on graphene surface coating and/or modification for wider biomedical applications.

System and methods

The sequence of the amyloid β-peptide fragment 33–42 ($A\beta_{33-42}$ – GLMVGGVVIA) features seven hydrophobic residues, making it a prime candidate for adsorption onto a highly hydrophobic graphene surface. Accordingly, this system was prepared for MD simulation as follows. An initial conformation of $A\beta_{33-42}$ was extracted from the solution structure of the Aβprotein (17–42), (PDB ID: 2BEG). An $A\beta_{33-42}$ monomer was first solvated in a cubic box with an edge length of 50 Å. Three independent 160 ns simulations were then performed to investigate the conformational diversity of $A\beta_{33-42}$ in solution. As a result, the peptide was found to assume β-hairpin structures to some extent in all three simulations.

Next, we studied the absorption of several $A\beta_{33-42}$ peptides onto a graphene monolayer and their subsequent interactions. Five peptides initialized in β-hairpin configurations were placed above a graphene sheet (58×58 Å^2 in dimension). The initial height of the center of mass of peptide with respect to the graphene is 7.4 Å. At the start of the simulations, all peptides were separated by at least 20 Å in center of mass (COM) (Fig. 1a). The size of solvation box is $59 \times 59 \times 45$ Å^3 with ~15 200 atoms. Subsequently, both replica exchange molecular dynamics (REMD)[42] and conventional molecular dynamics simulations of the system were performed. For the REMD simulations, we started 32 system replicas at temperatures exponentially distributed between 300 and 500 K. Each replica was propagated for 100 ns in simulation time. Attempts at exchange between neighboring replicas were conducted every 2 ps with the observed acceptance ratio varied between 12.3% and 29.2%. The conventional MD simulation was allowed to run for 1640 ns.

To better study the formation of adsorbed peptide assemblies, five $A\beta_{33-42}$ segments were started in fully coextensive configurations and assigned labels A through E. The three central peptides (B, C, and D) were placed with an inter-peptide COM separation of 7.5 Å and restrained to their initial positions by harmonic potential, whereas peptides A and E were retained to the extended configuration by imposing distance restraint between terminal residues. The two distal peptides (A and E) were then initialized at three progressively larger distances (12.5, 14.5 and 16.5 Å) from the central complex.[43] And the graphene sheet with larger size (101×102 Å^2 in dimension) was used. Each such starting configuration was generated in both parallel and antiparallel packing modes, yielding six systems in total for simulation. The starting configurations described here are illustrated in Fig. 3. The size of solvation box is $103 \times 104 \times 45$ Å^3 with ~47 500 atoms. For each system, five independent MD runs were performed to comprehensively study the approach and association of the two distal peptides to the central complex.

We also employed REMD simulations to study the stabilities of specially constructed parallel and antiparallel assemblies containing five extended peptides. The central peptide (C) was restrained to its initial position by harmonic potential while the remaining peptides were retained to the extended configuration by imposing distance restraint between terminal residues. The size of graphene sheet and solvation box is similar to the adsorption simulation. Each replica was allowed to run for 50 ns with the same replica number, temperature, and exchange parameters used as those described above.

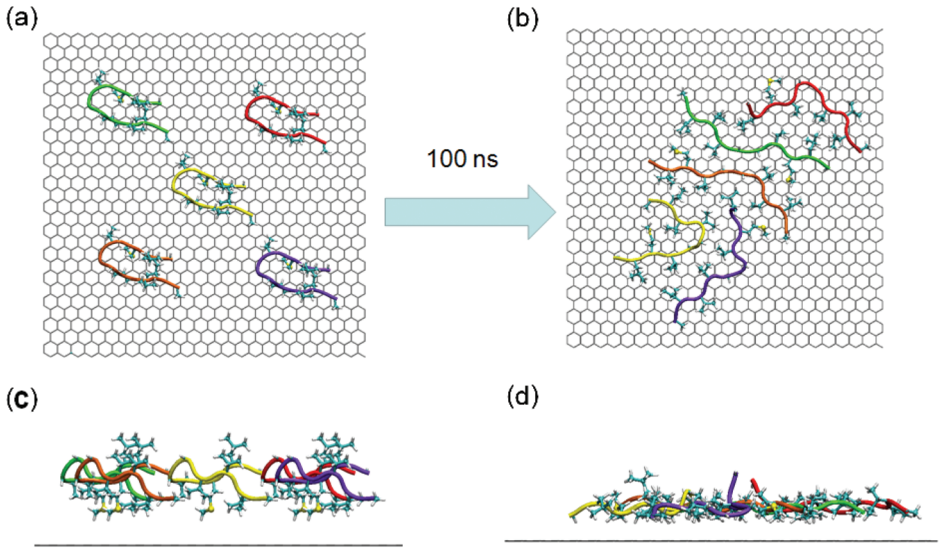

Fig. 1 The initial (a, c) and final structures (b, d) of five $A\beta_{33-42}$ peptides on graphene: 100 ns REMD simulation.

Moreover, we computed the free energy (potential of mean force, PMF) of peptide dissociation to estimate the binding stability of the adsorbed peptide assembly. The Adaptive Biased Force (ABF) method[44] was employed to calculate the free energy profile of the detachment of one peptide from the adsorbed assembly. The reaction coordinate was set to be the *z*-coordinate of Cα atom of either N- or C-terminal residue. For each system, 5 independent simulations were used to construct the free energy profile, thus overall, we performed 20 simulations to estimate the stability of both parallel and anti-parallel assembly. The resolution of reaction coordinate is 0.1 Å and the force constant is 10 kcal mol^{-1} A^{-2}.

All MD simulations were carried out using the NAMD 2.8 program in concert with the CHARMM27 force field.[45] Periodic boundary conditions were applied in all three coordinate directions. In all cases, dynamics were sampled from the canonical NVT ensemble (T = 300 K); temperature was modulated by a Langevin thermostat with a damping coefficient of 1 ps^{-1}. van der Waals interactions were treated using a switching function with twin-range cutoff distances of 10 and 12 Å. A cutoff distance for short-range electrostatic interactions was set at 12 Å; long range electrostatic interactions were treated with the particle mesh Ewald (PME) method.[46] All configurations were solvated using the TIP3P water model,[47] and all simulation snapshots were rendered with the program VMD.[48]

Results

To understand the structural ensemble of $A\beta_{33-42}$ in solution, we first analyze three independent 160 ns trajectories in the absence of a graphene surface. Starting from extended conformations, the largely hydrophobic peptide fragment exhibits a clear tendency to form collapsed structures: in each simulation, the peptide's radius of gyration (R_g) dramatically decreases from ~9 Å to ~5.5 Å (Fig. S1a†). In particular, the peptide is found to adopt a β-hairpin like structure (Fig. S2†) in all three trajectories. The root mean square deviation (RMSD) of the peptide with respect to a reference hairpin structure drops and remains below 2 Å in each simulation (Fig. S1b†). As such, this β-hairpin solution structure is deemed representative, and is used to initialize the simulations of peptide adsorption.

Starting each peptide in this β-hairpin structure, the adsorption and successive assembly of five $A\beta_{33-42}$ fragments onto a graphene monolayer was then probed using a 100 ns REMD simulation (*i.e.* peptide adsorption-assembly simulation). When first placed parallel to the graphene sheet at an initial height of 7.4 Å, the peptides exhibit a remarkable tendency to adsorb onto the graphitic surface (Fig. 1). The average number of peptide heavy atoms that contact with the graphene (with a distance < 4.5 Å) increases to around 360, a threefold increase over the course of the simulation. Furthermore, the average separation between the peptide atoms and the surface decreases to 4.5 Å (Fig. 2) by the end of the simulation. Consequently, we see that most peptide atoms come into contact with the graphene surface, a property well consistent with experimental observations of adsorbed peptide monolayers featuring heights of ~0.4 nm.[49] Drying between the hydrophobic residues prevalent in $A\beta_{33-42}$ and the aromatic surface undoubtedly drives the observed adsorption.

After adsorption, the peptides interact with one another and assemble into a dense, mosaic-like structure on the graphene surface. The average number of contacted atom pairs (here a contacted pair means the distance between atoms is smaller than 4.5 Å) increases dramatically as the simulation proceeds (Fig. S3†), and the mean observed radius of gyration increases considerably as the peptides assume extended conformations (Fig. S4†). Notably, strong interactions with the surface appear to pull residual side-chains into relatively flat

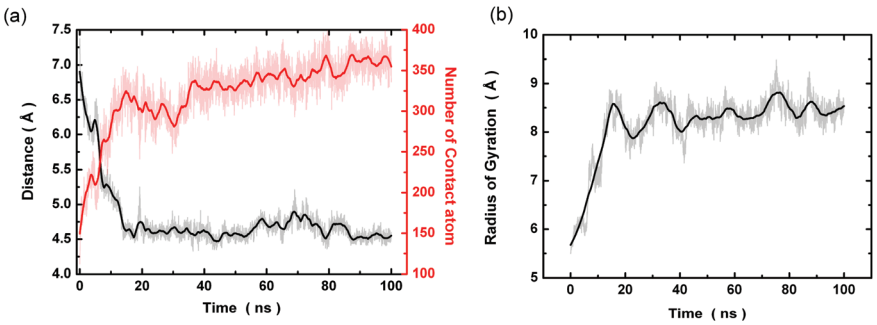

Fig. 2 (a) The averaged COM distance between the peptides and the graphene sheet (black) and the number of peptide heavy atoms contact with the graphene surface (red). (b) The average radius of gyration (R_g) of the peptides. Smoothed data (thicker line) are added for reference.

configurations arrayed on both sides of the adsorbed peptides (see Fig. 1 and S4† for illustrative examples). Such configurations prohibit the formation of backbone hydrogen bonds between the adsorbed peptides, implying that interactions within the adsorbed structure, stabilized by surface interactions, are dominated by hydrophobic attraction among the peptide side-chains. As a notable example, the two peptides shown in green and orange (Fig. 1, S4†) adopt linear configuration and are parallel to each other. Moreover, their side-chains interlock to form a hydrophobic interaction region on the graphene surface. The average backbone separation between these two peptides is around 7.6 Å. It should also be noted that even though the peptides undergo considerable diffusion on the surface, such mosaic-like assemble is largely retained.

To further validate our observations, we also performed a 1.6 μs conventional molecular dynamics simulation of the peptides' adsorption dynamics. The peptides associate with the graphene in a fashion similar to that observed above; however, the tendency of peptides to adhere strongly to the surface and assume extended configurations was comparatively modest (Fig. S5†). The average number of peptide heavy atoms found to be in contact with the graphene was about 220, and the mean vertical separation between the peptides and the surface was slightly larger (5.5 Å – see Fig. S6†). The mean peptide radius of gyration was also smaller than the one observed in the REMD simulation, fluctuating between 5.8 and 6.5 Å in the conventional simulation trajectory (Fig. S7†). Even though this investigation of the adsorption and conformational change of peptides by conventional simulation was less efficient, the mosaic-like motif of interactions among the adsorbed peptides was largely conserved in this trajectory (see Fig. S5 and S8†).

As suggested by the REMD and conventional MD simulations, $A\beta_{33-42}$ peptides thus appear to quickly and efficiently adsorb onto graphene surfaces. Subsequently, the peptide fragments form complexes featuring extended backbones and well packed arrays of hydrophobic side-chains. Notably, two of the peptides even spontaneously aligned into a near-parallel configuration. Given greater computational resources, one might seek to characterize the formation of better-defined peptide assembly structures in larger systems and at longer simulation times.

To further study the formation of peptide assemblies, we constructed six systems in both parallel and antiparallel configurations (Fig. 3). The peptides were prepared in linear conformations featuring a flattened and stretched array of side-chains, as inspired by our observation of a near-parallel peptide configuration in the above REMD simulation. Interestingly, experiments with our collaborators suggest that the adsorbed peptide monolayer consists of molecular nanostripes with a periodicity of ~2.8 nm, a distance comparable to the length of a fully extended $A\beta_{33-42}$ peptide.[49] It should be noted that Ramachandran angles corresponding to the prepared systems are consistent with standard β-strand configurations. The hydrophobic side-chains of Leu-2, Val-4, Val-7, and Val-9 of the adjacent peptides interlock nicely in both the parallel and antiparallel packing structures. The three central peptides (B, C, and D) were restrained to their initial position, whereas two distal peptides (A and E) were initialized at three progressively larger distances (12.5, 14.5 and 16.5 Å) from the central complex.

In the parallel-packed assemblies, the peptides placed at 12.5 Å (in all 5 independent simulation runs) and 14.5 Å (in 4 out of 5 runs, Fig. 3b) separations quickly approach the peptide complex in the middle. The distance between peptides A–B and D–E decreases to around 7.5 Å, close to the fixed separation between peptide pairs B–C and C–D. The number of contacting atoms between peptide pairs A–B and D–E also increases to a level comparable to that seen between the restrained central peptide pairs (Fig. S9 and S10†). Once more, it appears that hydrophobic interactions between stretched side-chains serve to promote the association of the peptides under observation. The final side-chain packing between peptide pairs A–B and D–E is consistent with packing among the central peptides, suggesting that the hydrophobic interaction regions are important for spontaneous assembly (Fig. 3b).

In cases of an even larger initial separation (16.5 Å), simultaneous association of the peptides A and E to the central complex was only observed in one simulation (Fig. S11†). In other simulations, one of the two free peptides fails to

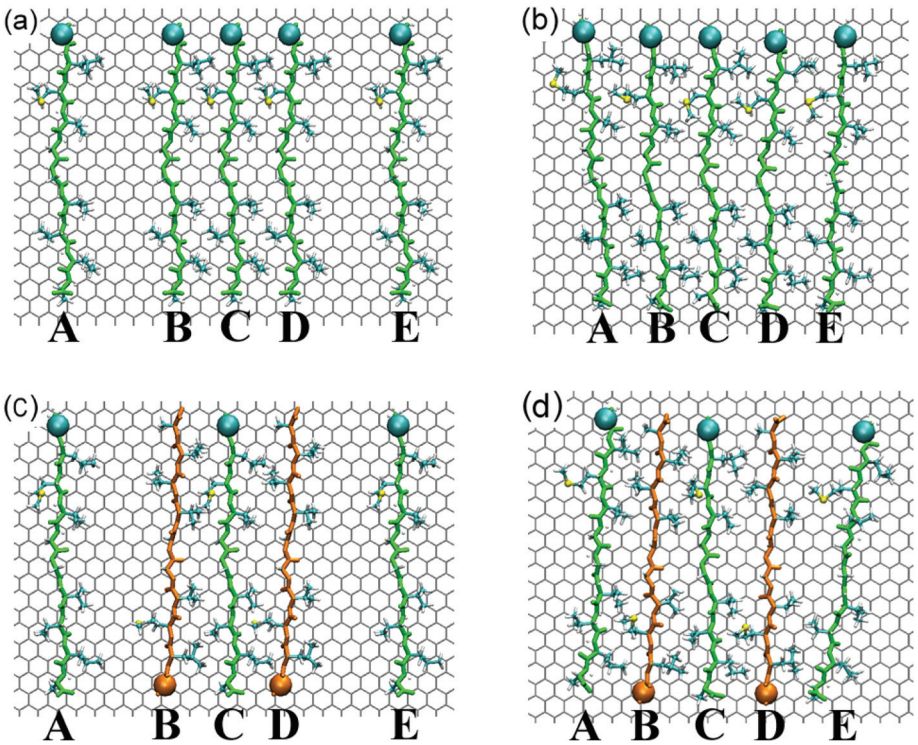

Fig. 3 The formation of peptide assemblies: the initial (a, c) and final structure (b, d) of five $A\beta_{33-42}$ peptides on graphene. The peptides are denoted as A, B, C, D, E, respectively (from left to right). The assemblies of both parallel (a, b) and antiparallel (c, d) packing structure are shown. The peptides at both ends are initially placed with 14.5 Å separation: *i.e.*, 7 Å larger than the fixed peptide separation.

associate with the restrained assembly. This large initial separation may have exceeded the length threshold corresponding to the dramatic association of peptides observed at shorter separations.

In the antiparallel assembly, peptides placed at a 12.5 Å initial separation also quickly approach the central peptide complex. The stretched hydrophobic side-chains contact and interlock to form the hydrophobic interaction regions seen in the restrained antiparallel structure. Association from an initial 14.5 Å separation, however, was only successful in one antiparallel simulation (see Fig. 3d), no spontaneous assembly in systems starting with the most extreme separation (16.5 Å) was observed. Considered in tandem, peptides placed in both parallel and antiparallel arrangements exhibit a tendency to approach and add to the specific assembly structures we have proposed. Formation of such structures in the parallel packing assembly, however, seems to be more efficient than under antiparallel packing motif.

Though these peptides adopt β-strand-like structures, the observed peptide assembly is quite distinct from the one formed through ordinary β-sheet assembly. First, the strand separation (~7.5 Å) seen in the above complex is considerably larger than expected in standard β-sheet assemblies (~5 Å). In stark contrast to almost all β-sheet structures, backbone hydrogen bonds are thus prohibited in the surface-bound β-strand complex. The formation of this well-structured β-strand assembly on a graphitic surface, therefore, can be mainly attributed to a patchwork of interactions among the hydrophobic side-chains.

We further studied these unique adsorbed assemblies *via* REMD simulation by constructing well-packed, five-peptide assemblies in both parallel and antiparallel configurations on a graphene surface. Both assemblies largely maintain their structures during simulation, and adjacent peptides maintain their contacts for the most part. Relative peptide positions and specific contacts do fluctuate, however, particularly in the antiparallel-packed complex. Fig. 4 shows representative configurations of both complexes obtained from the last 1 ns trajectory of the 300 K replica. The mean number of contacting atom pairs between all pairs of adjacent peptides is substantially larger (107.3) in the parallel case as compared to the one in the antiparallel complex (75.1), implying a relative deficit in stability for antiparallel packing. On the other hand, the interaction between peptides may be mediated by the water molecules which simultaneously form hydrogen bonds with adjacent peptides. We found water molecules can form some limited "bridging" hydrogen bonds between adjacent peptides within adsorbed assembly (Fig. S12†). And the average number of water-mediated hydrogen bonds (the number of water molecules simultaneously form hydrogen bonds with adjacent peptides) for parallel-packed and anti-parallel packed complex is only 1.17 and 0.84, respectively. In other words, the stability of peptide assembly should be largely attributed to the hydrophobic side-chain interactions.

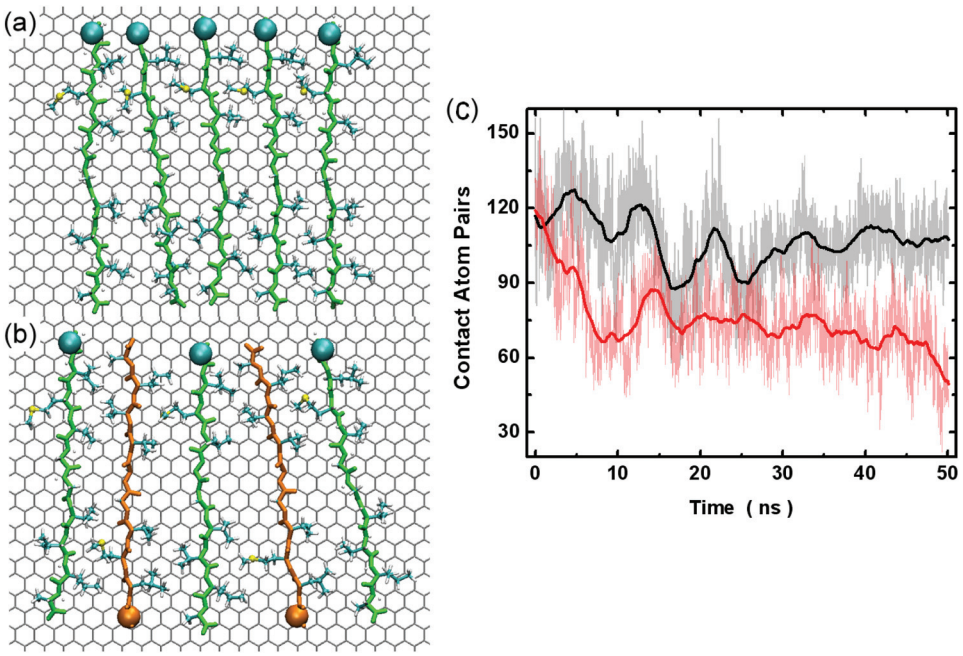

Fig. 4 The stability of peptide assemblies: (a, b) representative configurations of peptide assemblies (featuring parallel and antiparallel packing structures) taken from the final 1 ns trajectories of the REMD simulation. (c) The number of contacting atom pairs between adjacent peptides for the assemblies with parallel (black) and antiparallel packing structure (red). The smoothed data (thicker line) are added.

Similar properties were observed in another REMD simulation of the adsorbed five-peptide assemblies in which the three peptides in the middle (*i.e.* peptide B, C, D) were restrained to their initial positions and peptides A and E were free to move (Fig. S13†). In the parallel-packed complex, the number of contacting atom pairs between peptides A–B and D–E remained at around 57, and the peptides A and E retained fully extended configurations. By contrast, the number of contacting atom pairs decreases in the antiparallel case, and the configuration of peptides A and E underwent considerable fluctuation. The enhanced stability of parallel, fully extended peptide configurations is once more in line with the experimental observations of ~2.8 nm-wide peptide nanostripes, a width consistent with the length of fully extended $A\beta_{33-42}$ peptides.

Even though the size of peptide assemblies included in the simulations is limited, our results (Fig. 4 and S13†) suggest that this distinct form of surface-bound β-strand assembly, maintained by hydrophobic side-chain interactions, is quite stable. We also find that the stability of such a β-strand assembly is sensitive to its packing arrangement, paralleling the characteristics of ordinary β-sheet assembly. This finding is supported by the experimental results based on Fourier transform infrared spectroscopy (FT-IR).[49] In addition, we evaluated the stability of surface-bound assembly by computing the free energy of dissociation of one peptide from the assembly using Adaptive Biased Force (ABF) method (Fig. S14†). The peptide was detached *via* both its N- and C-terminus. In the case of parallel assembly, the free energy of N- and C-terminus detachment is −62.0 and −60.5 kcal mol^{-1}, respectively. As for the antiparallel assembly, the corresponding free energy is −59.5 and −58.8 kcal mol^{-1}, respectively. The stability of such surface-bound assembly can be attributed to the hydrophobic interaction with graphitic surface as well as the adjacent peptide, and it is comparable to the Aβ assembly connected by backbone hydrogen bonds.[50]

As indicated above, the formation and stability of this non-canonical form of peptide assembly can be mainly attributed to hydrophobic interactions between side-chains of the adsorbed peptides. Stabilized by surface interactions, this hydrophobic attraction is evidently strong enough to induce and maintain the assembly structure. As stretched hydrophobic side-chains form a mosaic of specific hydrophobic interaction regions in the complex, the complementarity in side-chain size and shape within this patchwork should be crucial to its stability. The hydrophobic residues present in $A\beta_{33-42}$ (*i.e.* Met, Val, Leu, Ile) share a similar size with three or four heavy atoms present in each respective side-chain. Accordingly, the stretched side-chains of these residues can smoothly interlock over the graphitic surface. The side-chain of Met is comparatively long, making Met-3 a better fit between Leu-2 and Val-4 than between Val-7 and Ile-9 (Fig. S15†). This steric factor may contribute to higher structural stability observed within the parallel packing β-strand assembly.

This surface-adsorbed, patchwork form of β-strand assembly may also be realized by other peptides composed of hydrophobic residues with side-chains of complementary size. Interestingly, peptide segments meeting this criterion can be found in several other proteins, *e.g.* $\alpha\text{-synuclein}_{66-78}$, $\text{prion}_{113-125}$, and IAPP_{8-17}, among others. Further studies

concerning whether these peptide segments can form patchwork β-strand assemblies when adsorbed are certainly warranted. In a reciprocal sense, the design of peptides which can similarly adsorb and assemble on hydrophobic surfaces also presents an interesting problem.

Conclusion

In this work, we report the formation of a distinct type of β-strand assembly and discuss results concerning its stability and mechanism of association. We find that $A\beta_{33-42}$ peptides will quickly adsorb onto a graphene surface and exhibit a tendency to adopt extended β-strand structures. The adsorbed peptides can interact with each other and form β-strand assembly on the graphene. Interestingly, the structures of these assemblies are distinct from normal β-sheets, as interactions with graphene facilitate hydrophobic side-chain interactions among peptides. Given the mosaic-like patchwork formed by these side-chains, complementarity in side-chain size and shape is likely important for stabilizing this type of β-strand assembly. Hence, our simulation results reveal a unique β-strand assembly, maintained by hydrophobic side-chain interactions rather than backbone hydrogen bond. Hence, this structure is distinct to both "free standing" and other adsorbed peptide assemblies previously reported, where the peptides within adsorbed assembly are still connected by backbone hydrogen bonds even though the surface interaction can indeed affect the assembly process and mesoscopic architecture. Our current findings about β-strand assembly suggest backbone hydrogen bond is no longer crucial to peptide assembly. The prospect that such β-strand assemblies could be realized by other peptides in biologically relevant contexts is exceptionally exciting. Further study of surface-induced peptide assembly should deepen our understanding of how peptide assemblies formed on membranes and more generic surfaces, a subject that promises to have immense applications to medical biology and materials science. Furthermore, these studies may also help advance the development of nanotechnology on surface coating/modification of nanomaterials.

Acknowledgements

This work is supported by the 100-Talent Project from the Chinese Academy of Science, the Ministry of Science and Technology (MOST) 973 program 2013CB933704, 2012CB932504 and the National Natural Science Foundation of China (NSFC) grants 21273240. R.Z. acknowledges financial support from IBM Blue Gene Science Program.

References

1 C. M. Dobson, *Trends Biochem. Sci.*, 1999, **24**, 329.
2 C. Soto, *Nat. Rev. Neurosci.*, 2003, **4**, 49.
3 C. M. Dobson, *Nature*, 2003, **426**, 884.
4 F. Chiti and C. M. Dobson, *Annu. Rev. Biochem.*, 2006, **75**, 333.
5 J. Schnabel, *Nature*, 2010, **464**, 828.
6 M. Goedert and M. G. Spillantini, *Science*, 2006, **314**, 777.
7 F. T. Arce, H. Jang, S. Ramachandran, P. B. Landon, R. Nussinov and R. Lal, *Soft Matter*, 2011, **7**, 5267.
8 T. Luhrs, C. Ritter, M. Adrian, D. Riek-Loher, B. Bohrmann, H. Dobeli, D. Schubert and R. Riek, *Proc. Natl. Acad. Sci. U. S. A.*, 2005, **102**, 17342.
9 Q. Li, L. Liu, S. Zhang, M. Xu, X. Wang, C. Wang, F. Besenbacher and M. Dong, *Chem. – Eur. J.*, 2014, **20**, 7236.
10 Q. Wang, N. Shah, J. Zhao, C. Wang, C. Zhao, L. Liu, L. Li, F. Zhou and J. Zheng, *Phys. Chem. Chem. Phys.*, 2011, **13**, 15200.
11 T. Kowalewski and D. M. Holtzman, *Proc. Natl. Acad. Sci. U. S. A.*, 1999, **96**, 3688.
12 X. Yu, Q. Wang, Y. Lin, J. Zhao, C. Zhao and J. Zheng, *Langmuir*, 2012, **28**, 6595.
13 L. Dusan, L. M. Lisandra, A. Marie-Isabel and H. S. David, *Pept. Sci.*, 2006, **84**, 519.
14 M. J. McMasters, R. P. Hammer and R. L. McCarley, *Langmuir*, 2005, **21**, 4464.
15 A. Karsai, L. Grama, U. Murvai, K. Soó s, B. Penke and M. S. Z. Kellermayer, *Nanotechnology*, 2007, **18**, 345102.
16 X. Mao, Y. Guo, C. Wang, M. Zhang, X. Ma, L. Liu, L. Niu, Q. Zeng, Y. Yang and C. Wang, *ACS Chem. Neurosci.*, 2011, **2**, 281.
17 I. Brovchenko, G. Singh and R. Winter, *Langmuir*, 2009, **25**, 8111.
18 Y.-P. Yu, S. Zhang, Q. Liu, Y.-M. Li, C. Wang, F. Besenbacher and M. Dong, *Soft Matter*, 2012, **8**, 1616.
19 J. Guo, J. Li, Y. Zhang, X. Jin, H. Liu and X. Yao, *PLoS One*, 2013, **8**, e65579.
20 S.-g. Kang, T. Huynh, Z. Xia, Y. Zhang, H. Fang, G. Wei and R. Zhou, *J. Am. Chem. Soc.*, 2013, **135**, 3150.
21 X. Mao, Y. Guo, Y. Luo, L. Niu, L. Liu, X. Ma, H. Wang, Y. Yang, G. Wei and C. Wang, *J. Am. Chem. Soc.*, 2013, **135**, 2181.
22 L. Ou, Y. Luo and G. Wei, *J. Phys. Chem. B*, 2011, **115**, 9813.
23 C. R. So, Y. Hayamizu, H. Yazici, C. Gresswell, D. Khatayevich, C. Tamerler and M. Sarikaya, *ACS Nano*, 2012, **6**, 1648.
24 Y. Sheng, W. Wang and P. Chen, *J. Phys. Chem. C*, 2010, **114**, 454.
25 W. Yang, Q. Ren, Y.-N. Wu, V. K. Morris, A. A. Rey, F. Braet, A. H. Kwan and M. Sunde, *Biopolymers*, 2013, **99**, 84.
26 H. A. Lashuel and P. T. Lansbury, *Q. Rev. Biophys.*, 2006, **39**, 167.
27 N. Arispe, H. B. Pollard and E. Rojas, *Proc. Natl. Acad. Sci. U. S. A.*, 1993, **90**, 10573.
28 A. Quist, I. Doudevski, H. Lin, R. Azimova, D. Ng, B. Frangione, B. Kagan, J. Ghiso and R. Lal, *Proc. Natl. Acad. Sci. U. S. A.*, 2005, **102**, 10427.
29 G. Valincius, F. Heinrich, R. Budvytyte, D. J. Vanderah, D. J. McGillivray, Y. Sokolov, J. E. Hall and M. Loche, *Biophys. J.*, 2008, **95**, 4845.

30 M. R. de Planque, V. Raussens, S. A. Contera, D. T. Rijkers, R. M. Liskamp, J. M. Ruysschaert, J. F. Ryan, F. Separovic and A. Watts, *J. Mol. Biol.*, 2007, **368**, 982.
31 C. Cheng, S. Li, J. Zhao, X. Li, Z. Liu, L. Ma, X. Zhang, S. Sun and C. Zhao, *Chem. Eng. J.*, 2013, **228**, 468.
32 E. Gazit, *Chem. Soc. Rev.*, 2007, **36**, 1263.
33 X. Zhao, F. Pan, H. Xu, M. Yaseen, H. Shan, C. A. E. Hauser, S. Zhang and J. R. Lu, *Chem. Soc. Rev.*, 2010, **39**, 3480.
34 S. Emamyari and H. Fazli, *Soft Matter*, 2014, **10**, 4248.
35 C. Li and R. Mezzenga, *Nanoscale*, 2013, **5**, 6207.
36 X. Mao, Y. Wang, L. Liu, L. Niu, Y. Yang and C. Wang, *Langmuir*, 2009, **25**, 8849.
37 L. Xie, Y. Luo, D. Lin, W. Xi, X. Yang and G. Wei, *Nanoscale*, 2014, **6**, 9752.
38 S. Assenza, J. Adamcik, R. Mezzenga and P. D. L. Rios, *Phys. Rev. Lett.*, 2014, **113**, 268103.
39 T. P. Knowles, A. W. Fitzpatrick, S. Meehan, H. R. Mott, M. Vendruscolo, C. M. Dobson and M. E. Welland, *Science*, 2007, **318**, 1900.
40 J. Adamcik and R. Mezzenga, *Macromolecules*, 2012, **45**, 1137.
41 T. P. J. Knowles and M. J. Buehler, *Nat. Nanotechnol.*, 2011, **6**, 469.
42 K. Hukushima and K. Nemoto, *J. Phys. Soc. Jpn.*, 1996, **65**, 1604.
43 W. Han and K. Schulten, *J. Am. Chem. Soc.*, 2014, **136**, 12450.
44 E. Darve and A. Pohorille, *J. Chem. Phys.*, 2001, **115**, 9169.
45 J. A. MacKerell, D. Bashford, M. Bellott, R. L. Dunbrack, J. D. Evanseck, M. J. Field, S. Fischer, J. Gao, H. Guo, S. Ha, D. Joseph-McCarthy, L. Kuchnir, K. Kuczera, F. T. K. Lau, C. Mattos, S. Michnick, T. Ngo, D. T. Nguyen, B. Prodhom, W. E. Reiher, B. Roux, M. Schlenkrich, J. C. Smith, R. Stote, J. Straub, M. Watanabe, J. Wiórkiewicz-Kuczera, D. Yin and M. Karplus, *J. Phys. Chem. B*, 1998, **102**, 3586.
46 T. Darden, D. York and L. Pedersen, *J. Chem. Phys.*, 1993, **98**, 10089–10092.
47 J. Tirado-Rives and W. L. Jorgensen, *Biochemistry*, 1991, **30**, 3864–3871.
48 W. Humphrey, A. Dalke and K. Schulten, *J. Mol. Graphics*, 1996, **14**, 33.
49 L. Liu, Q. Li, S. Zhang, X. Wang, S. V. Hoffmann, J. Li, F. Besenbacher and M. Dong, *ACS Nano*, 2015, submitted.
50 J. A. Lemkul and D. R. Bevan, *J. Phys. Chem. B*, 2010, **114**, 1652.

